Modelling Micro-Rheological Effects in Micro Injection Moulding with Dissipative Particle Dynamics

D. Kauzlarić, A. Greiner and J. G. Korvink

Institute for Microsystem Technology, University of Freiburg, Germany, kauzlari@imtek.de

ABSTRACT

We investigate the applicability of Dissipative Particle Dynamics for the rheological study of fluids in micro-cavities, e.g., for micro injection moulding. For this purpose, we have simulated Poiseuille flow, i.e., pressure drive flow and varied the driving force and the gap width. The obtained average velocities and shear viscosities show that Newtonian behaviour of our fluid can be observed up to a certain limit of the strength of the driving force and is approached by increasing the gap width. Measured density profiles show that downscaling leads to density fluctuations in a natural way, which are not covered by continuum approaches without additional terms in the equations of motion. As an example of a more complex geometry, flow passing a backward facing micro-step was simulated.

Keywords: injection moulding, Poiseuille flow, Newtonian flow limit, density fluctuations, dissipative darticle dynamics

1 INTRODUCTION

Micro Injection Moulding (Micro-IM) of polymers is a promising process technology for low cost production with high throughput of high-quality 3D electronic or mechanical micro-components. The moulds represent the most expensive part of the production costs. Therefore, once designed and fabricated, the mould must fulfil all requirements.

A well designed mould allows for good filling by the feedstock. Therefore, software tools are necessary in order to predict the filling behaviour. This should include prediction of the necessary pressure for complete filling, investigation of the transient temperature behaviour, detection of slip or jetting.

There exist many promising continuum approaches based on the Navier-Stokes equations (see e.g. [1, 2, 3]). But still, many of the mentioned requirements are missing because the original intention was the simulation of macroscopic Polymer-IM, i.e., the developers did not explicitly represent the microscale effects appearing in Micro-IM.

On a molecular level, Molecular Dynamics (MD) [4, 5] represents an attractive simulation technique for the study of hydrodynamic phenomena. Already for injection moulding in geometries with sizes in the range of several tenths of micrometers, practical computational speed demands a sort of coarse graining of the molecular model. An attractive technique to fulfil this requirement is Dissipative Particle Dynamics (DPD) [6].

2 DISSIPATIVE PARTICLE DYNAMICS

DPD discretizes the continuum into point particles. The positions and momenta of the particles are updated in a continuous phase space at discrete time steps. The updates are computed by applying Newton's second law for a particle of mass m_i

$$\frac{d\mathbf{r}_i}{dt} = \frac{\mathbf{p}_i}{m_i}, \quad \frac{d\mathbf{p}_i}{dt} = \mathbf{F}_i^{ext} + \sum_{j,j\neq i} \mathbf{f}_{ij} \tag{1}$$

with $\mathbf{r}_i$ and $\mathbf{p}_i$ being the position and momentum vector of particle i. $\mathbf{F}_i^{ext}$ is an external force field acting on each particle. $\mathbf{f}_{ij} = \mathbf{F}_{ij}^D + \mathbf{F}_{ij}^R + \mathbf{F}_{ij}^C$ is a pair force between two particles i and j. $\mathbf{F}_{ij}^D$ is a dissipative force, $\mathbf{F}_{ij}^R$ is a stochastic force, and $\mathbf{F}_{ij}^C$ is a conservative force.

For $\mathbf{F}_{ij}^D$ and $\mathbf{F}_{ij}^R$ suitable forms, which fulfil Galilean invariance, are

$$\mathbf{F}_{ij}^D = -\gamma\omega_D(r_{ij})(\mathbf{e}_{ij}\cdot\mathbf{v}_{ij})\mathbf{e}_{ij} \tag{2}$$

and

$$\mathbf{F}_{ij}^R = \sigma\zeta_{ij}\omega_R(r_{ij})\mathbf{e}_{ij}. \tag{3}$$

The vector $\mathbf{e}_{ij} = \mathbf{r}_{ij}/r_{ij}$ is the unit vector pointing from particle j to particle i. $\mathbf{v}_{ij} = \mathbf{v}_i - \mathbf{v}_j$ is the relative velocity between the particles. ζ_{ij} is a random number with the properties $\langle\zeta_{ij}(t)\rangle = 0$ and a delta correlation $\langle\zeta_{ij}(t)\zeta_{kl}(t')\rangle = (\delta_{ik}\delta_{jl} + \delta_{il}\delta_{jk})\delta(t-t')$. γ can be interpreted as a friction coefficient and σ is a noise amplitude. $\omega_D(r_{ij})$ and $\omega_R(r_{ij})$ are weight functions determining the range of the forces and their strength as a function of the

interparticle distance r_{ij}. For $r_{ij} \geq r_c$ these functions vanish, with r_c being the cutoff distance.

For a well-defined equilibrium temperature, detailed balance requires a fluctuation-dissipation theorem for DPD to be fulfilled [7], which is:

$$\omega_D(r_{ij}) = \omega_R^2(r_{ij}) \text{ and } \frac{2k_B T}{m}\gamma = \sigma^2 \tag{4}$$

m is the mass of a particle, k_B is the Boltzmann constant and T stands for the equilibrium temperature. Usually, the weight functions are chosen to be

$$\omega_D(r_{ij}) = \omega_R^2(r_{ij}) = \begin{cases} \left(1 - \frac{r_{ij}}{r_c}\right)^2, & r_{ij} < r_c \\ 0, & r_{ij} \geq r_c \end{cases} \tag{5}$$

A convenient choice for the conservative force is [8]

$$\mathbf{F}_{ij}^C = a\,\omega_R(r_{ij})\mathbf{e}_{ij} \tag{6}$$

with a representing the amplitude.

Equation (1) is integrated numerically over a small time step Δt. For integration we use the modified Velocity-Verlet algorithm as described in [8].

As is common practice in MD or DPD, dimensionless units are used for the quantities needed for computation.

3 SIMULATION SETUP

For the study of the bulk behaviour of a DPD-fluid, periodic boundary conditions (PBC) are usually applied, i.e., a particle leaving the simulation box at one side reenters the domain at the opposite end. Additionally, our simulations need the introduction of walls. They are modelled by introducing stochastic thermalizing boundary conditions (STBC).

"Stochastic" means that the direction in which a particle colliding with the wall is reflected back into the box is drawn randomly, with a mean velocity of zero parallel to the wall. This corresponds to a no-slip boundary condition.

"Thermalizing" means that the wall represents a large thermal reservoir. Every particle is reflected back into the box with a velocity drawn from a Maxwell-Boltzmann distribution corresponding to the defined temperature.

For a wall in the y-direction, this behaviour can be realised by drawing the velocity component v_y from a Rayleigh distribution

$$\Phi(v_y) = \frac{m}{k_B T_w} v_y \exp\left(-\frac{m v_y^2}{2k_B T_w}\right) \tag{7}$$

and v_x and v_z from a Maxwell distribution

$$\Phi(v_i) = (2\pi m k_B T_w)^{-\frac{1}{2}} \exp\left(-\frac{m v_i^2}{2k_B T_w}\right) \tag{8}$$

with zero mean. The index i is a placeholder for x or z and T_w stands for the wall temperature. In all simulations, the wall temperature is set to $T_w = T_{fluid} = 1$.

With slight modifications this mechanism was already used earlier by others for boundary conditions at walls in Couette flow (see e.g. [9]).

Initially, the particles possess a mean velocity of zero in all Cartesian directions. The initial configuration of the particles is a simple cubic lattice with lattice constant $l_a = \rho^{-1/3}$ determined from the particle density ρ. This is valid if we assume the mass of all particles to be $m = 1$. The symmetry vanishes very rapidly during simulation and does not affect the results presented here.

In order to generate pressure driven flow, a constant force f_x is exerted on each particle. Here, the assumption from continuum theory is adopted that a constant force field leads to a linear pressure gradient. Because of $m = 1$, each particle is accelerated equally with $g_x = f_x / m$.

4 SIMULATION RESULTS

4.1 Dependencies on driving force

Poiseuille flow was simulated in several runs for a system of $N_p = 2000$ particles. The dimensions of the simulation box were chosen to be $l_x = l_y = 20 l_a$ and $l_z = 5 l_a$, l_y being the gap width, i.e., the distance between the two walls. Following Groot and Warren [8] we have chosen $\sigma = 3$, $\rho = 3$ and $a = 25$.

The results indicate Newtonian behaviour of the DPD-fluid for $g_x \leq 0.06$ and shear thickening above. For larger driving forces, the slope of $\langle\langle v_x \rangle(t)\rangle(g_x)$, i.e., of the steady flow average velocity as a function of the driving force (see Fig. 1), decreases.

The shear viscosity η was estimated from the velocity profiles using the analytical expression for the velocity profile in the flow direction for Poiseuille flow [10]:

$$v_x(y) = \frac{\rho g_x l_y^2}{2\eta}\left(y - y^2\right) \tag{9}$$

The cross-stream coordinate y is normalised such that $0 \leq y \leq 1$, with $y = 0$ and $y = 1$ representing the two walls, respectively. We observe a constant shear viscosity

for $g_x \leq 0.06$ and an increase for bigger forces, i.e., shear thickening. Equation (10) assumes laminar flow and a constant density.

Fig. 2 shows plots of the relative density $\rho_{rel} = \rho / \langle \rho \rangle$ over the cross-stream coordinate y for $g_x = 0.005$ and $g_x = 0.32$.

We can see that the density seems to be constant over a wide range of the channel. At the walls, there are large fluctuations and equation (9) is definitely not valid anymore. In Fig. 3 we zoom in on the ordinate to densities $0.85 < \rho_{rel} < 1$. Here, we can see that the density for $g_x = 0.005$ is really constant for a sufficient distance from the walls and despite the fluctuations due to the finite number of particles.

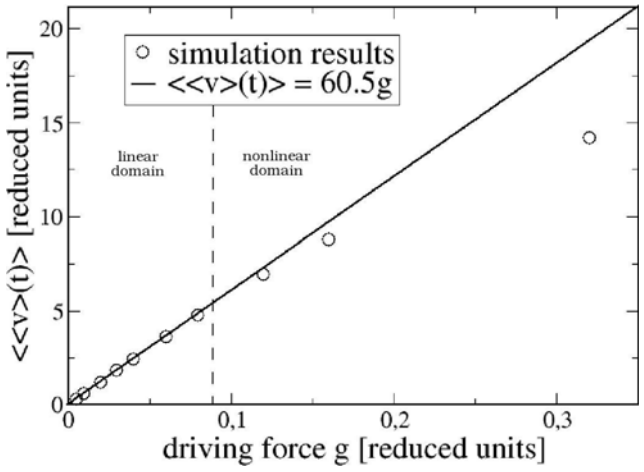

Fig. 1: Plot of $\langle\langle v_x \rangle(t)\rangle$ as a function of g_x. Additionally, the function $\langle\langle v_x \rangle(t)\rangle = 60.5 g_x$ is plotted for comparison.

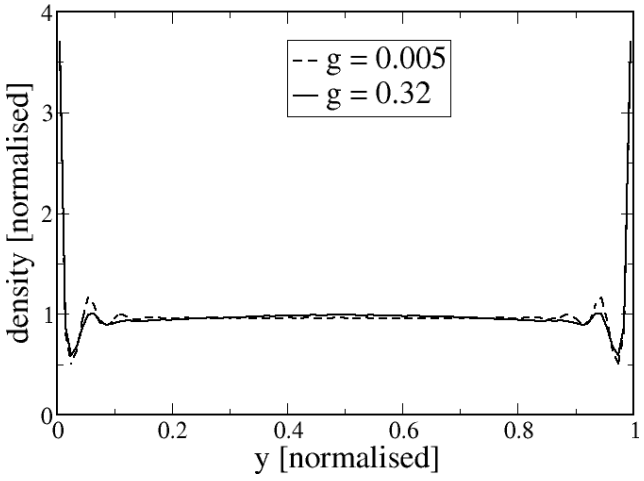

Fig. 2: Cross-stream density profile for the simulation runs with $g_x = 0.03$ and $g_x = 0.32$.

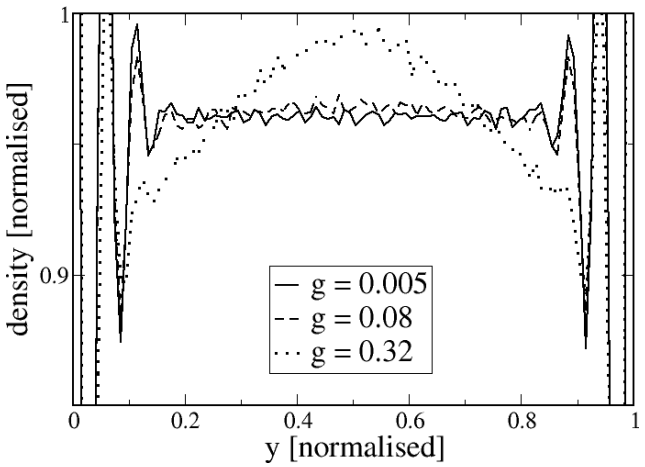

Fig. 3: Density profile. Zoom into the range $0.85 < \rho_{rel} < 1$.

But for large driving forces, we can see a "buckling" of the density profile, which sets in very close to the driving force, for which the fluid starts to behave nonlinearly (see fig. 1).

4.2 Dependencies on gap width

Additional simulation series were performed for gap widths l_y of $10 l_a$, $40 l_a$, $60 l_a$ and $80 l_a$.

In Fig. 4 the density at the walls is plotted as a function of the gap width for $g_x = 0.01$, which is always in the linear domain. The density seems to converge to $\rho_{rel} = 1$ for an increasing gap width. This can be considered as an increase of the characteristic length in our simulation domain. In this case, the representation of the fluid remains constant. The other possibility is to consider the variation of l_y as a variation of the particle resolution, i.e., the number of particles representing the same amount of fluid.

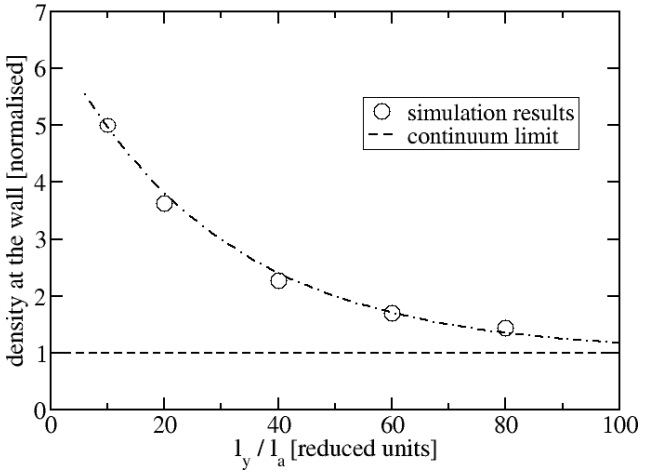

Fig. 4: Maximum relative density ρ_{rel} at the walls as a function of the gap width.

In any case, the results indicate convergence to the continuum limit for $l_y \to \infty$.

4.3 Flow in a step geometry

A DPD-fluid passing a backward facing step was simulated. Snapshots are shown in Fig. 5. This test geometry is used to determine the effect of jetting, which occurs in the injection moulding process. At high solidification rates, this effect leads to a large amount of weld lines or even trapped air pockets [11]. One of the goals of this work is to be able to predict these effects.

In a first experiment, the step height was chosen to be $10l_a$, which is half of the gap width of the outlet. Several empirical observations are made: (i) This simple fluid model has a low viscosity, i.e. the Reynolds number is too large for a feedstock. (ii) No stable flow front can be established which is due to the purely repulsive conservative force $\mathbf{F}_{ij}^{C}$ used in this model (see equation (6)). Further work is concentrated on these two challenges.

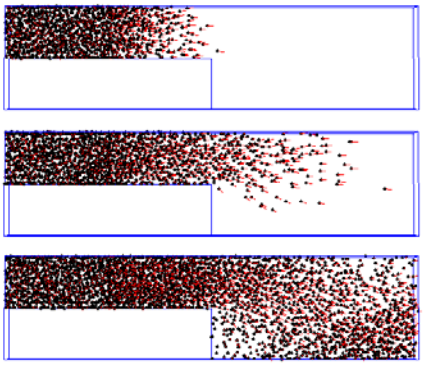

Fig. 5: DPD-fluid passing a backward facing step

5 CONCLUSIONS

The presented results show that DPD can reproduce continuum theory in the domains where it is valid. Additionally DPD delivers microrheological information, which is not accessible with the continuum approach.

Strictly spoken, the viscosity derived from continuum theory is wrong, since it assumes a constant density of the fluid. This is not really a problem, but rather underlines what we want to show: by down-scaling the simulated dimensions, we reach domains where continuum approaches, as, e.g., equation (9), produce wrong results. The computed velocities are inherent to the model, i.e., they are correct for the model. They converge to the continuum results for the right choice of simulation parameters. In our case this means a decrease of the driving force under a certain threshold and an increase of the system size.

We therefore conclude that the deviation from the continuum solution is a deviation from bulk behaviour, which again is due to the increasing influence of down scaling and surface effects. We see these deviations since the DPD-method is able to model these effects naturally, which have to be added separately as corrections in continuum approaches [3].

6 ACKNOWLEDGEMENTS

Financial support by the German research association (DFG) in the framework of the special research area SFB 499 is gratefully acknowledged. Additionally, the contribution of Mr. J. Bardong (IMTEK) to the computational measurements is gratefully acknowledged.

REFERENCES

[1] T. Barriere and J. C. Gelin, Journal de Physique 11(4), 248, 2001
[2] C. A. Hieber and S. F. Shen, J. Non-Newt. Fluid Mech. 7, 1, 1980
[3] D. Yao and B. Kim, J. Micromech. Microeng. 12, 604, 2002
[4] D. C. Rapaport, "The Art of Molecular Dynamics Simulation", Cambridge University Press, 1995
[5] J. M. Haile, "Molecular Dynamics Simulation. Elementary Methods", Wiley Interscience, 1997
[6] P. J. Hoogerbrugge and J. M. V. A. Koelman, Europhys. Lett. 19(3), 155, 1992
[7] P. Español and P. Warren, Europhys. Lett 30(4), 191, 1995
[8] R. D. Groot and P.B. Warren, J. Chem. Phys. 107(11), 4423, 1997
[9] C. Trozzi and G. Ciccotti, Physical Review A 29(2), 916, 1984.
[10] L.D. Landau, and E.M. Lifshitz, "Fluid Mechanics", Pergamon Press, 1959
[11] R. M. German and A. Bose, "Injection Molding of Metals and Ceramics", Metal Powder industries Federation Princeton, 1997